OncoTargets and Therapy

Dovepress
open access to scientific and medical research

Open Access Full Text Article

ORIGINAL RESEARCH

Lipid–Polymer Hybrid Nanoparticle-Based Combination Treatment with Cisplatin and EGFR/HER2 Receptor-Targeting Afatinib to Enhance the Treatment of Nasopharyngeal Carcinoma

This article was published in the following Dove Press journal:
OncoTargets and Therapy

Dehui Fu
Chao Li
Yongwang Huang

Department of Ear-Nose-Throat (ENT), The Second Hospital of Tianjin Medical University, Tianjin, 300211, People's Republic of China

Purpose: Nasopharyngeal carcinoma (NPC) is one of the most prevalent carcinomas among the Cantonese population of South China and Southeast Asia (responsible for 8% of all cancers in China alone). Although concurrent platinum-based chemotherapy and radiotherapy have been successful, metastatic NPC remains difficult to treat, and the failure rate is high.

Methods: Thus, we developed stable lipid–polymer hybrid nanoparticles (NPs) containing cisplatin (CDDP) and afatinib (AFT); these drugs act synergistically to counter NPC. The formulated nanoparticles were subjected to detailed in vitro and in vivo analysis.

Results: We found that CDDP and AFT exhibited synergistic anticancer efficacy at a specific molar ratio. NPs were more effective than a free drug cocktail (a combination) in reducing cell viability, enhancing apoptosis, inhibiting cell migration, and blocking cell cycling. Cell viability after CDDP monotherapy was as high as 85.1%, but CDDP+AFT (1/1 w/w) significantly reduced viability to 39.5%. At 1 μg/mL, AFT/CDDP-loaded lipid–polymer hybrid NPs (ACD-LP) were significantly more cytotoxic than the CDDP+AFT cocktail, indicating the superiority of the NP system.

Conclusion: The NPs significantly delayed tumor growth compared with either CDDP or AFT monotherapy and were not obviously toxic. Overall, the results suggest that AFT/CDDP-loaded lipid–polymer hybrid NPs exhibit great potential as a treatment for NPC.

Keywords: nasopharyngeal carcinoma, cisplatin, afatinib, nanoparticles, antitumor, apoptosis

Introduction

Nasopharyngeal carcinoma (NPC), a malignancy of the nasopharyngeal epithelium, is one of the most prevalent carcinomas among the Cantonese population of South China and Southeast Asia (responsible for 8% of all cancers in China alone).[1] NPC invades locally and can then metastasize to lymph nodes and other distant organs. Given such high invasiveness, most patients are diagnosed at advanced stages, which are associated with a poor prognosis.[2] Radiotherapy is one of the major treatment options for drug-sensitive non-metastatic NPC. Advances in imaging and radiotherapy have improved the 5-year survival rate of non-metastatic NPC patients to 76.7%; however, treatment failure is more common in patients with metastatic NPC.[3] It is believed that over 90% of NPCs are undifferentiated and might respond

Correspondence: Yongwang Huang
Department of Ear-Nose-Throat, The Second Hospital of Tianjin Medical University, No. 23 Pingjiang Road, Tianjin, 300211, People's Republic of China
Tel/Fax +86 22-88328701
Email ywhuanghss@163.com

submit your manuscript | www.dovepress.com
DovePress
http://doi.org/10.2147/OTT.S286813

to chemotherapy if diagnosed early. Despite the great improvement in survival, 20–30% of the patients are still at risk of treatment failure because of distant metastases, emphasizing the urgent need for effective treatments.[4,5]

Platinum-based dual chemotherapy (cisplatin, CDDP) is the standard treatment regimen for metastatic NPC.[6] Presently, CDDP combined with continuous 5-fluorouracil infusion is widely used to treat metastatic NPC. However, the response is short-lived, and mucosal complications limit the clinical benefits.[7] Therefore, a new platinum-based combination chemotherapy is needed to improve the therapeutic outcome, with minimal toxicity. The epidermal growth factor receptor (EGFR) is a member of the ERBB family of receptors overexpressed in several epithelial malignancies including NPC.[8] EGFR overexpression and hyperactivation are directly correlated with tumor resistance and a poor prognosis. Several therapies focused on EGFR inhibition have been developed to modulate cancer resistance and improve treatment effectiveness.[9] Monoclonal antibodies (such as cetuximab and nimotuzumab) and tyrosine kinase inhibitors (TKIs) against EGFR have been therapeutically effective in preclinical and clinical research, but no benefits were evident in a large proportion of clinical patients.[10,11] It has been reported that 75–90% of NPC cases exhibit EGFR overexpression; however, EGFR mutations are rarely observed, indicating that EGFR mutations may not play roles in NPC.[12] This explains why first-generation TKIs (gefitinib and erlotinib) have only been effective in NPC patients with EGFR mutations, and not the general patient population.[13]

It has been reported that the human epidermal growth factor (HER2) receptor, another ERBB receptor, may heterodimerize with EGFR and thus alter the subsequent signaling pathways.[14,15] Alternatively, overexpression and heterodimerization of the HER2 receptor may eliminate any need for activation of EGFR to initiate downstream signaling. Based on the reports, we thus hypothesized that overactivation of HER2 may limit the clinical benefits afforded by EGFR-based therapies and that more effective therapies are required.[16–19] Compared with the first-generation TKIs, afatinib (AFT) potently inhibits all kinases of the ERBB family including mutant and wild-type EGFR and HER2.[20] Compared with gefitinib and erlotinib, which bind reversibly to the ATP-binding site of EGFR, AFT irreversibly (covalently) binds to ERBB family members and completely blocks signaling.[21,22] In this study, we combined a platinum agent (CDDP) with AFT (an EGFR/HER2 inhibitor) and found that they acted synergistically against NPC.

Chemotherapy exhibits immense potential in vitro but often fails when given systemically. Wide drug biodistributions to normal organs and immediate clearance from the blood cause some of the serious side effects of free drugs.[23] Nanomedicine has attracted a great deal of attention because it seeks to encapsulate drugs to improve therapeutic outcomes. Nanoparticles (NPs) of a certain size range passively enter the tumor vasculature via enhanced permeation and retention (EPR).[24] Thus, lipid–polymer (LP) hybrid NPs featuring a biodegradable hydrophobic core surrounded by a phospholipid monolayer ideally encapsulate pairs of drugs.[25] To improve the efficacy of NPC therapy, we loaded CDDP and AFT into LP NPs. We performed extensive in vitro tests using human NPC cells (the HONE1 line) and explored in vivo efficacy using a murine xenograft model.

Materials and Methods

Preparation of AFT/CDDP-Loaded LP Hybrid NPs (ACD-LP NPs)

Poly(DL-lactide-co-glycolide) (PLGA), AFT, and CDDP were purchased from Sigma-Aldrich (China). 1,2-dilauroyl-sn-glycero-3-phosphocholine (DLPC) and 1,2-distearoyl-sn-glycero-3-phosphoethanolamine-N-[amino(polyethylene glycol) (DSPE-PEG) 2000] were purchased from Avanti Polar Lipids (China). AFT (20 mg), CDDP (20 mg), and PLGA (150 mg) were dissolved in DCM (an organic solvent) and stirred well to form an oil phase. Separately, DSPE-PEG (100 mg) and DLPC (150 mg) were dissolved in 1% (w/v) poloxamer solution to form an aqueous phase. The oil phase was added to the aqueous phase in a dropwise manner with continuous mechanical stirring at 1000 rpm for 10 min. The mixture was immediately sonicated (with a probe) for 5 min and then stirred for 3 h to remove all organic solvent. The NP suspension was centrifuged at 12,000 rpm for 8 min, and the pellet was washed three times with ultrapure water. The amounts of AFT and CDDP loaded into NPs were measured. A Waters 2998 photodiode array UV/visible detector and a μRPC C2/C18 ST 4.6/100 column were used to assay AFT, whereas an ICP-mass spectrometry platform (Agilent 7700; Agilent Technologies, Japan) fitted with an EnyaMist nebulizer (Burgener, Ontario, Canada) was employed to detect CDDP. For AFT, the mobile phase consisted of 10 mM ammonium acetate (pH 6.7) (solvent A) and acetonitrile (ACN) (solvent B); the elution gradient was linear: 0 min

10% B; 5 min 50% B, 7 min 80% B, 10 min 80% B, 11 min 10% B, and 12 min 10% B, respectively.

Nanoparticle Characterizations

The particle characteristics including particle size distribution, polydispersity index (PDI) and surface charge was determined using Zeta PALS instrument (Brookhaven Instruments, Austin, TX, USA) by dynamic light scattering principle. The samples were prepared by diluting the NP dispersions with ultrapure water to particle count of 300 and then measurements were performed at 25±1°C. All the measurements were recorded in triplicate. The morphology was examined using JEOL 100CX transmission electron microscope (TEM; Tokyo, Japan). Briefly, a drop of freshly diluted nanoparticle dispersion was deposited onto a 300-mesh copper grid coated with carbon and dried at room temperature. Followed by a drop of 2% phosphotungstic acid was added and excessive solution was removed using a filter paper and observed under the TEM.

In vitro Drug Release Study

In vitro release profile of AFT and CDDP from ACD-LP was examined in pH 7.4 and pH 5.0 buffer conditions using diffusion technique. Freeze-dried NPs were dispersed in 1 mL of respective pH 7.4 or pH 5.0 buffer containing an equivalent of 1 mg/mL of ART And CDDP. The dialysis membrane (MWCO 3500) was sealed from both the end and dialyzed against 30 mL of buffer with a constant stirring speed of 100 rpm at 37°C for 72 h. At predetermined time interval, 1 mL of release buffer was withdrawn and replenished with equal volume of new respective buffer. The released buffer is divided into two equal parts with one part is used for the ART determination and the other part was used for the estimation of CDDP. The released drug concentration was expressed as a percentage of total drugs in the NPs and plotted as a function of time. The representative AFT and CDDP analysis has been presented in Figure S1.

In vitro Cellular Uptake

Human nasopharyngeal carcinoma cells (HONE1) cell were obtained from China Type Culture Collection and Cancer Research Center (Wuhan, China), and C666-1 was purchased from cell bank of Chinese Academy of Sciences (Shanghai, China). Cells were cultured in RPMI1640 medium supplemented with 10% of fetal bovine serum (FBS) with 1% antibiotic mixture. For cellular uptake analysis, HONE1 cells were seeded in a 6-well plate and incubated for 24 h. The cells were then exposed with ACD-LP-loaded with Rhodamine B as a fluorescent tracker for 1–3 h. The cells were then washed twice, extracted, centrifuged. Cells were examined for 10,000 counts under flow cytometer (BD FACS, Biosciences, USA).

Analysis of Cytotoxic Activity of Drug Combinations in HONE1 Cells

MTT (3-[4,5-dimethylthiazol-2-yl]-2,5-diphenyltetrazolium bromide) was performed to evaluate the cytotoxic potential of individual and combinational drugs. Briefly, HONE1 cells were seeded in 96-well plates at a density of 10,000 cells per well and incubated for 24 h. At first, cells were separately treated with free CDDP and free ART and incubated for 24 h. In order to examine the combination index (CI), cells were treated with various molar fractions of free CDDP and ART and incubated for 24 h. In order to evaluate the effect of nanoparticle-based drug encapsulation, cells were treated with a fixed concentration of free drugs, combination cocktail and dual-drug-loaded nanoparticles (ART-LP) and incubated for 24 h. Followed by, 20 µL of 5 mg/mL of MTT solution was added to the individual well and incubated for 4 h. The upper medium was discarded and 100 µL of DMSO was added to dissolve the formazan crystals and absorbance was read at 570 nm using a microplate reader (Plate CHAMELEON™ V-Hidex). Untreated cells were considered as an appropriate control. The mean drug concentration required for 50% growth inhibition (IC50) was determined using CompuSyn software (Version 1.0, Combo-Syn Inc., U.S.).

Combination Index (CI) was analyzed on HONE1 cell by the well-established Chou and Talalay method using CompuSyn software. For each value of Fraction Affected (Fa), the CI values of ART+CDDP combination were evaluated by the following equations;

$$CI = (D)1/(Dx)1 + (D)2/(Dx)2$$

whereas (D)1 and (D)2 are the concentrations of individual drug in the drug combination that results in Fa × 100% growth inhibition, while (Dx)1 and (Dx)2 are the concentrations of the drugs alone resulting in Fa × 100% growth inhibition. CI values CI>1, CI=1 and CI<1 corresponds to antagonistic, additive and synergistic effect.

Apoptosis Effect of Drug Combinations in HONE1 Cells

The apoptosis assay was performed in two ways; first, apoptosis of cancer cell was evaluated by Hoechst 33358 staining analysis. HONE1 cells were seeded in 96-well plates at a density of 10,000 cells per well and incubated for 24 h. The cells were treated with individual drugs as well as combinational drugs and incubated for 24 h. Complete culture medium was present in the untreated group and considered as control. Later, the cells were washed twice with PBS, fixed with 4% paraformaldehyde for 10 min and washed again. The washed cells were stained with Hoechst 33358 solution (10 µg/mL) at 37°C for 15 min in dark. The cells were washed twice with PBS carefully and observed under fluorescence microscope (IX71; Olympus, Japan). Second, apoptosis of cancer cells was evaluated using the double staining protocol of Annexin V-fluorescein isothiocyanate/propidium iodide (Annexin V-FITC/PI). The HONE1 cells were seeded in 96-well plates at a density of 10,000 cells per well and incubated for 24 h. The cells were treated with individual drugs as well as combinational drugs and incubated for 24 h. Then, cells were collected, centrifuged and pellet was re-dispersed using 50 µL of PBS. The cells were incubated with 2 µL of Annexin-V and 2 µL of PI each for 15 min. Early apoptotic cell is characterized by intact cell membrane but exposed phosphatidylserine that will bind to Annexin-V while late apoptotic cell is stained by both Annexin-V and PI. Cell-Quest software (BD Biosciences, San Jose, CA, USA) was used to calculate the apoptosis cells.

Cell Cycle Analysis

HONE1 cells were seeded in 6-well plates at a density of 20,000 cells per well and incubated for 24 h. Cells were treated with a fixed concentration of free drugs, combination cocktail and dual-drug-loaded nanoparticles (ART-LP) and incubated for 24 h. The cells were washed with ice-cold PBS, extracted and washed with PBS by centrifugation process. The cells were fixed with 70% ethanol overnight at 4°C. The ethanol was discarded from cells by centrifugation at 2000 rpm for 5 min at 4°C and washed with PBS using the same centrifugation process. Cells were then treated with RNAase (20 µg/mL) at 37°C for 30 min and then stained with PI (50 µg/mL) for 30 min at 4°C in dark atmosphere. The cells were subjected to flow cytometer (BD Biosciences, USA) to evaluate the distribution of cells in G0/G1, S, G2M and sub-G1 phase using FlowJo-V10/Cell Quest acquisition software (BD Biosciences).

Cell Migration Assay

Wound healing assay was performed to analyze the cell migration after treatment with respective formulations. HONE1 cells were seeded in 6-well plates at a density of 10,000 cells per well and incubated for 24 h. The cells were wounded using a plastic pipette tip and washed with PBS and replenished with culture medium. The images were observed at 0 h using Axiovert 200 M microscope (Zeiss) equipped with a CoolSNAP™ ES camera (Photometric®; Roper Scientific). After 24 h incubation, again images were taken using the camera and closures of wounds were evaluated using Metamorph® (V6.3; Molecular Devices Corp.).

In vivo Tumor Xenograft Studies

All animal studies followed the guidelines framed by the Committee on Cancer Research Guidelines of the Second Hospital of Tianjin Medical University, Tianjin. All animal experiments were approved by the Animal Ethical Committee of the Second Hospital of Tianjin Medical University. Reporting was in compliance with Animal Research: Reporting In Vivo Experiments (ARRIVE 2.0) guidelines.[26] Six-to-eight-week-old nude Balb/c mice weighing approximately 20–22 g were maintained in a pathogen-free environment with free access to food and water under a 12-h/12-h day/night cycle. To develop tumor xenografts, 1×10^7 HONE1 cells suspended in 150 µL culture medium were inoculated in the right flanks of the mice and grew into tumors 80–100 mm^3 in volume. The mice were randomly assigned to six groups of eight mice each: control, blank LP, AFT, CDDP, CDDP+AFT, and ACD-LP NPs. AFT and CDDP were given at 5 mg/kg. All formulations were administered intravenously (three injections spaced 3 days apart). The mice were regularly weighed, and any adverse effects were noted. On day 18, the mice were sacrificed and the tumors extracted and weighed. Tumor volume was calculated as volume (mm^3) = length × width × 0.5.

Statistical Analysis

Data were expressed as mean ± standard deviation. Statistical analyses were performed using SPSS Version 16.0 software (SSPS Inc., Chicago, IL, USA). A difference of $p<0.05$ was considered statistically significant.

Results and Discussion

Formulation and Physicochemical Characterization of ACD-LP NPs

In this study, we hypothesized that overactivation of HER2 limits the clinical benefits of EGFR-based therapies and that more effective therapies are required. AFT is a second-generation TKI that irreversibly inhibits EGFR/HER2/HER4 receptors and, when used with other chemotherapeutic drugs, enhances antitumor responses. A recent in vitro study showed that AFT in combination with CDDP significantly inhibited the growth and survival of five lines of human EGFR-wild-type head-and-neck squamous cell carcinomas (HNSCCs). Thus, we selected the combination of AFT and CDDP. Both drugs were loaded into LP NPs prior to detailed in vitro and in vivo analyses (Figure 1A). The average NP particle size was 138.2 ± 1.26 nm, and the size distribution was narrow (0.124 PDI). Particles smaller than 200 nm can enter tumor tissues (Figure 1B), and the EPR effect of the tumor microenvironment facilitates NP accumulation. Transmission electron microscopy revealed spherical particles with darker cores and lighter shells reflecting the presence of lipids and polymers in the shell and core (Figure 1C). The entrapment efficiencies for AFT and CDDP were 93.2 ± 1.28% and 91.4 ± 1.46%, respectively.

In vitro Drug Release

AFT and CDDP release from ACD-LP NPs was examined at pH 7.4 and pH 5.0 at 37°C over 72 h. The lower pH was tested because the pH of the tumor microenvironment is lower than that of the normal physiological environment (Figure 2). Controlled drug release was observed at both pH levels. No difference between the release of AFT and that of CDDP was evident at either pH; both drugs were preferentially released at pH 5.0. The similar release profiles may reflect the hydrophobic nature of both drugs and their loading into the cores of the NPs. Approximately ~30% of the drugs were released at pH 7.4 and ~40% at pH 5.0 over 24 h. No initial release burst was noted. The relatively lower release at pH 7.4 may minimize drug-related toxicities. The relatively higher release at pH 5.0 may enhance therapeutic efficacy after internalization into tumor tissue via the EPR effect.

Cellular Uptake and Cytotoxic Effects of the Drug Combination on HONE1 Cells

The internalization efficiency of drug-loaded NPs is key in terms of therapeutic efficacy. NPs enter cells via endocytosis, and the enclosed drugs are liberated in lysosomes. Flow cytometry revealed remarkable ACD-LP NP uptake by HONE1 cancer cells over time (Figure 3A). The cellular uptake was further confirmed with CLSM. As shown, ACD-LP showed a typical time-dependent cellular uptake as observed in HONE1 cells. A remarkable increase in the red fluorescence with time is indicative of the nanoparticle uptake in the cancer cells (Figure S2). Next, we examined the cytotoxic effects of free AFT and CDDP. AFT reduced cell viability to a significantly greater extent than did CDDP after 24 h of incubation. The IC50 value was calculated to compare the cell killing efficiency of individual drugs. The IC_{50} values of AFT and CDDP were 1.92 and 3.98 μg/mL, respectively (Figure 3B). Thus, CDDP+AFT combination therapy may greatly aid NPC management. Based on the IC50 value, we tested two drug combinations; the concentrations of both drugs were below the IC_{50} values (1 μg/mL) in one test and above the IC_{50} values in the second test (5 μg/mL). We varied the CDDP:AFT molar ratios (10/1, 2/1, and 1/1) at 1 and 5 μg/mL CDDP. Cell viability decreased with an increase in the molar ratio of CDDP:AFT (from 10:1 to 1:1; Figure 3C). Cell viability after CDDP monotherapy was 85.1%, whereas combination CDDP+AFT (1:1 w/w) yielded a significantly lower viability of 39.5%. Similar results were observed for CDDP at 5 μg/mL (53.6% viability for CDDP alone and 6.5% for the 1:1 [w/w] CDDP+AFT combination). Combination indices (CIs) were derived for the various molar ratios of CDDP and AFT. The principles of Chou and Talalay were applied using CompuSyn software. The combination indices for the 10:1, 2:1, and 1:1 drug ratios were 0.85, 0.45, and 0.21, respectively. The 1:1 CDDP+AFT combination was strongly synergistic, compared with CDDP alone and the other molar ratios. The 1:1 CDDP+AFT combination was used in all subsequent experiments. Based on this data, 1/1 molar ratio of CDDP and AFT was used to study the effect of nanoparticle carriers. At concentrations of 1 and 2.5 μg/mL, ACD-LP NPs exhibited a significantly higher cytotoxic effect compared with the CDDP+AFT cocktails, emphasizing the superiority of the LP NPs (Figure 3D). For example, the IC_{50} values of CDDP and AFT were 3.98 and 1.92 μg/mL, whereas that of the CDDP+AFT combination was 0.85 μg/mL. ACD LP NPs exhibited a significantly lower IC_{50} of 0.27 μg/mL. We have also studied the efficacy of free drugs and formulations in another EBV-positive nasopharyngeal cell

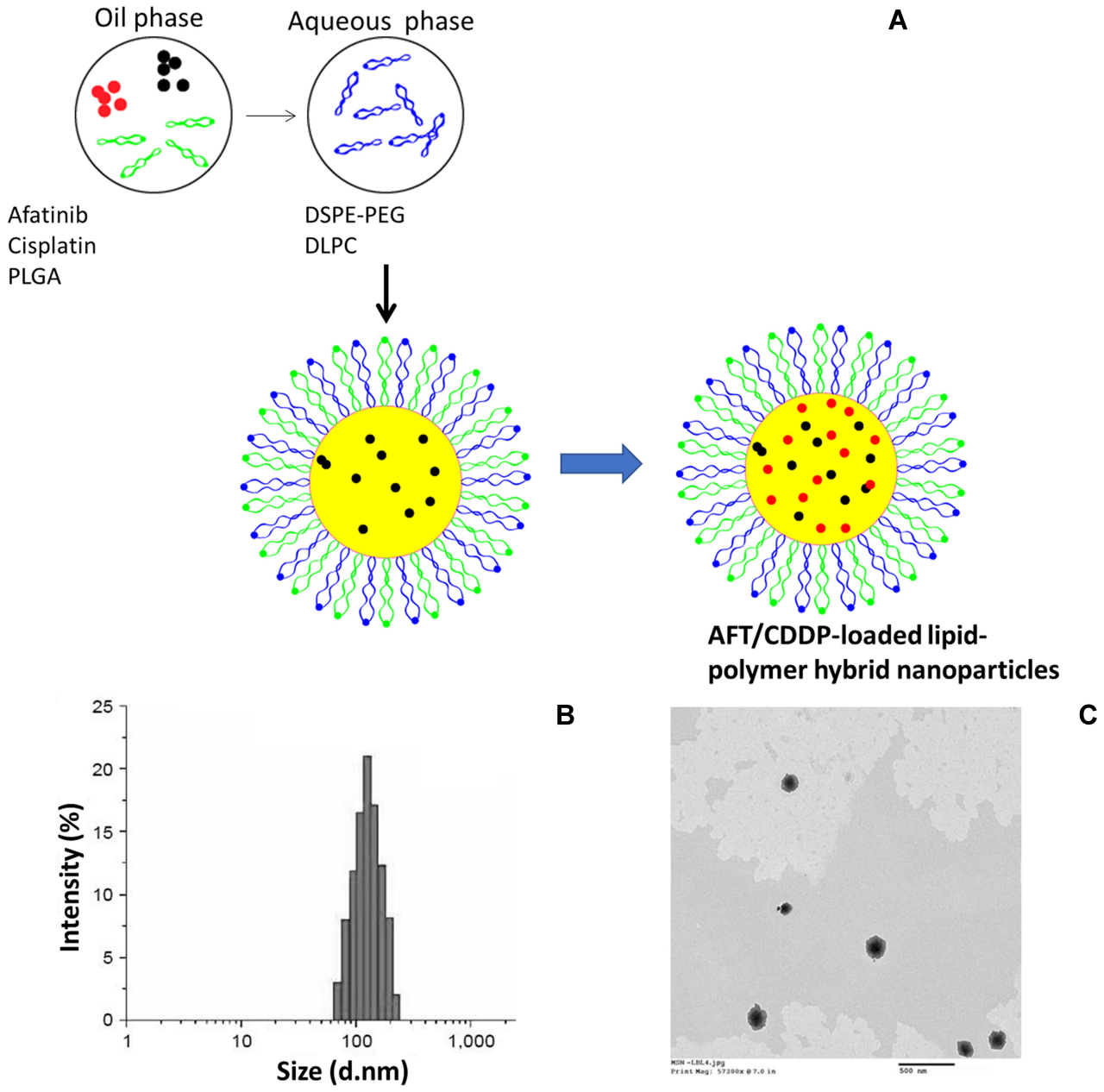

Figure 1 (**A**) A schematic of cisplatin- and afatinib-loaded lipid–polymer hybrid nanoparticles prepared via emulsification. (**B**) The particle size distribution as revealed by dynamic light scattering. (**C**) Nanoparticle morphology as revealed by transmission electron microscopy.

(C666-1). Similar efficacy was observed in C666-1 cells as observed in HONE1 cells. AFT and CDDP exhibited a concentration-dependent cytotoxic effect (Figure S3). Nanoparticle-based AFT-LP and CDDP-LP showed better cell killing effect compared to that of respective free drugs. Most importantly, combination drug-based ACD-LP showed significantly lower cell viability in C666-1 cells compared to that of either free drug cocktail or individual free drugs or individual nanoparticles indicating the synergistic activity of two drugs (Figure S4). Our findings clearly suggest that AFT may improve NPC treatment efficacy compared with CDDP monotherapy.

Apoptotic Effects of the Drug Combination on HONE1 Cells

The synergistic effects of CDDP and AFT on HONE1 cells were first investigated via Annexin-V/propidium iodide staining and flow cytometry. As shown in Figure 4, free CDDP and AFT induced apoptosis in 10–12% of cells and

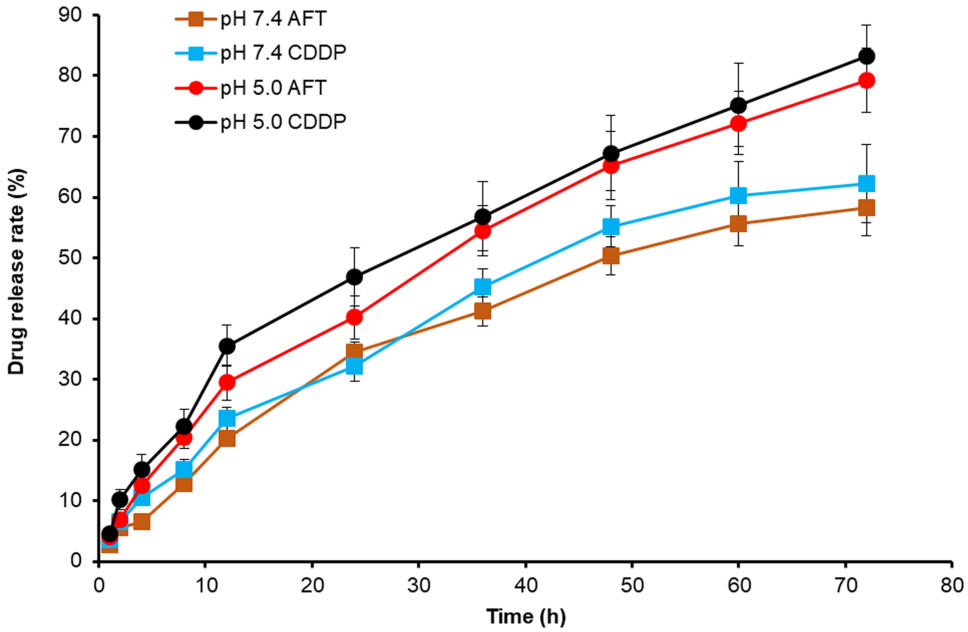

Figure 2 The release of cisplatin and afatinib from lipid–polymer hybrid nanoparticles over 72 h at pH 7.4 and pH 5.0. Afatinib was assayed via high-performance liquid chromatography and cisplatin via mass spectrometry.

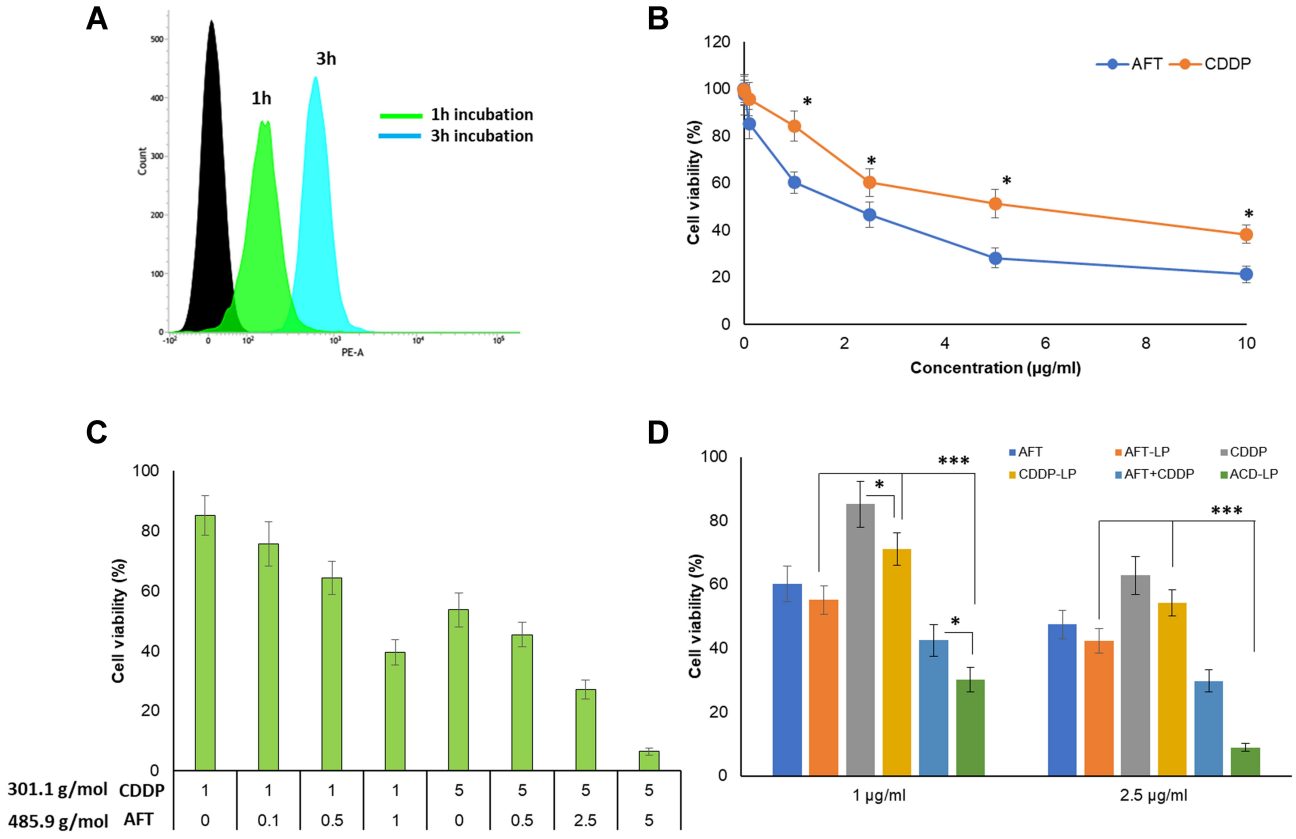

Figure 3 (**A**) Cellular uptake of cisplatin- and afatinib-loaded lipid–polymer hybrid nanoparticles by HONE1 cells as revealed by flow cytometry. (**B**) The viability of HONE1 cells. Concentration-dependent cytotoxicity was assayed using the MTT assay. (**C**) The effects of the drugs at different molar ratios on cell viability. (**D**) The effects of different formulations on cell viability. *p<0.05 and ***p<0.0001 is the statistical difference.

the CDDP+AFT cocktail in ~30% of cells. ACD-LP NPs exhibited a remarkably higher apoptosis rate, indicating a superior anticancer potential compared with the individual free drugs and the cocktail. We subjected cells to Hoechst 33258 staining. Cells exposed to free CDDP or AFT had smaller nuclei compared with the controls, but most cells were intact. Cells exposed to ACD-LP NPs exhibited a high level of apoptosis; the bright staining indicated nuclear condensation and fragmentation (typical of apoptosis). It has been reported that AFT decreases the levels of phospho-EGFR and phospho-HER2 and remarkably inhibits cancer cell proliferation and survival.[27,28] Downregulation of EGFR or HER2 directly inhibits PI3K/Akt/mTOR signaling, triggering apoptosis.[29,30] In NPC, CDDP treatment (alone)

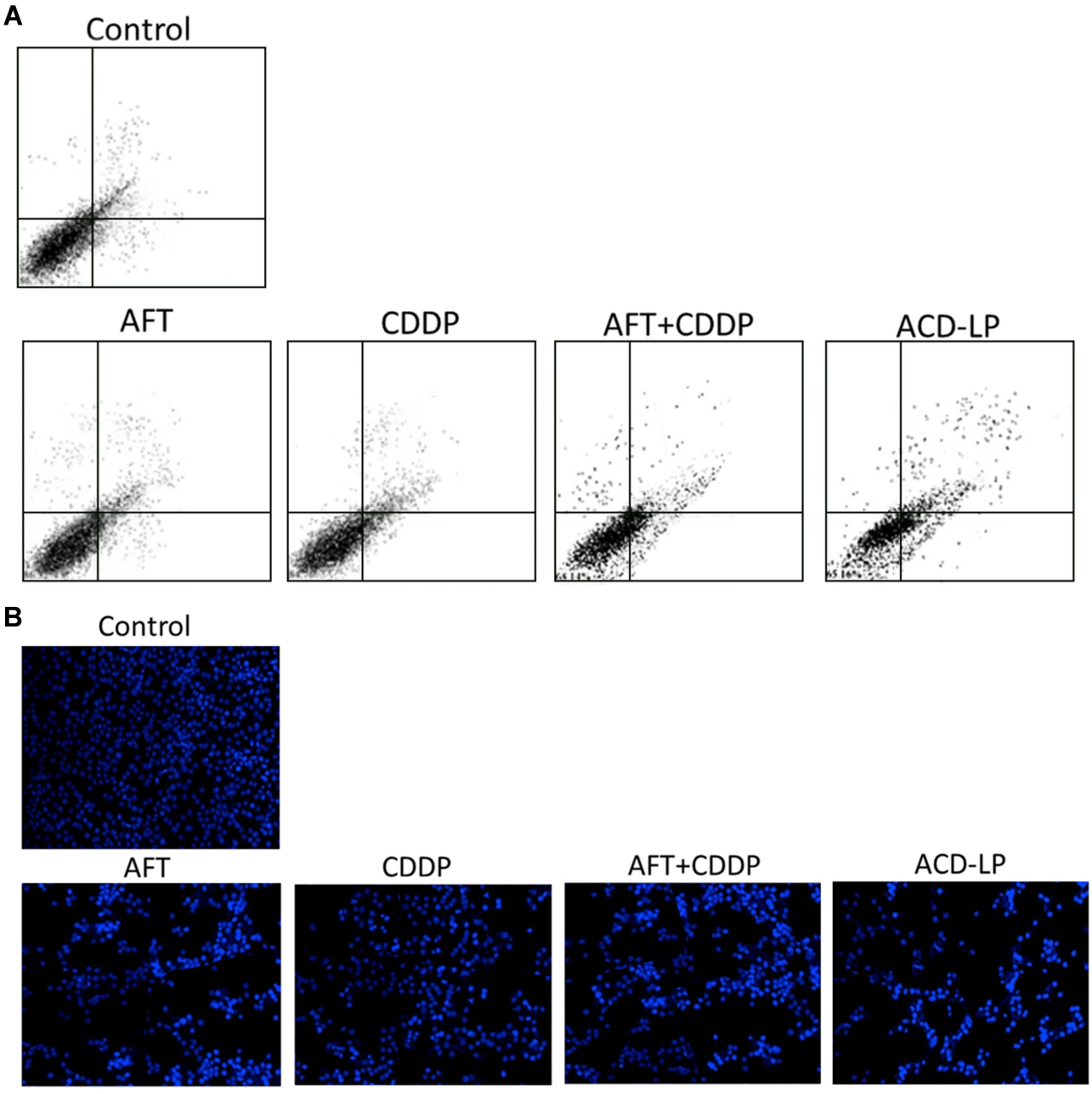

Figure 4 (**A**) Apoptosis of HONE1 cells as revealed by flow cytometry after staining with Annexin V-FITC and propidium iodide. (**B**) Qualitative analysis of apoptosis employing Hoechst 33258 staining. The free drugs (alone or in combination) and cisplatin- and afatinib-loaded lipid–polymer hybrid nanoparticles were incubated with cancer cells for 24 h.

resulted in greater cell viability (thus less apoptosis) compared with treatment with CDDP+AFT, and the effects were primarily attributable to inhibition of EGFR/HER2 co-expression and heterodimerization; downstream signaling was blocked.

Cell Cycle Analysis

The cell cycle distributions of HONE1 cells following administration of the single and combined regimens are presented in Figure 5. CDDP arrested the cell cycle at the G2/M phase; the CDDP+AFT cocktail increased the proportion of cells in the G2/M and sub-G0 phases (apoptosis) and decreased the proportion in the G0/G1 phase. ACD-LP NPs remarkably increased the proportion of cells in sub-G0 and decreased that in G2/M, suggesting the powerful anticancer efficacy of dual-drug-loaded LP NPs. Co-delivery of AFT and CDDP encapsulated in a nanocarrier increased cell cycle arrest and death compared with the cocktail or individual free drugs.

ACD-LP NPs Inhibited Cell Migration

NPC invades locally and then metastasizes to lymph nodes and other distant organs, resulting in a poor prognosis (Figure 6). We explored the effects of CDDP and AFT individually or in combination on NPC cell migration using a wound-healing assay. Untreated cells migrated freely, and treatment with CDDP or AFT alone did not effectively reduce migration. ACD-LP NPs greatly inhibited HONE1 cell migration because of the synergistic anticancer activity and the dual pharmacological pathways in play.

The Antitumor Efficacy of Combined Therapy in an NPC Xenograft Model and in vivo Toxicity

We examined the antitumor efficacy of single- and dual-drug-loaded NPs using an NPC xenograft model; the doses of CDP and AFT were both 5 mg/kg (Figure 7A). Empty LP NPs did not reduce the tumor burden compared with the untreated control. CDDP and AFT

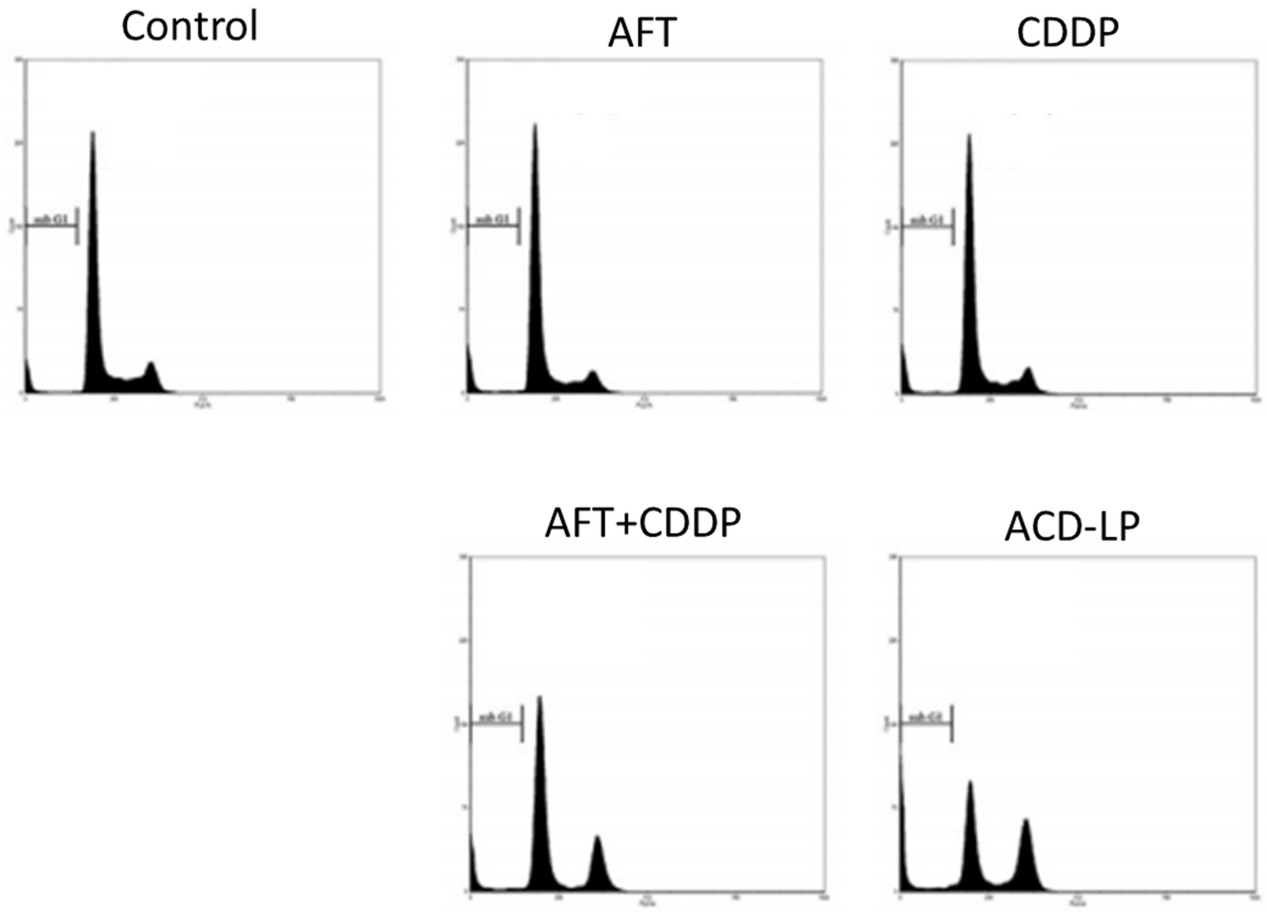

Figure 5 Cell cycle analysis of HONE1 cells using flow cytometry after staining with PI. The proportions of cells in the G0/G1, S, G2/M, and sub-G0 cell cycle phases were analyzed.

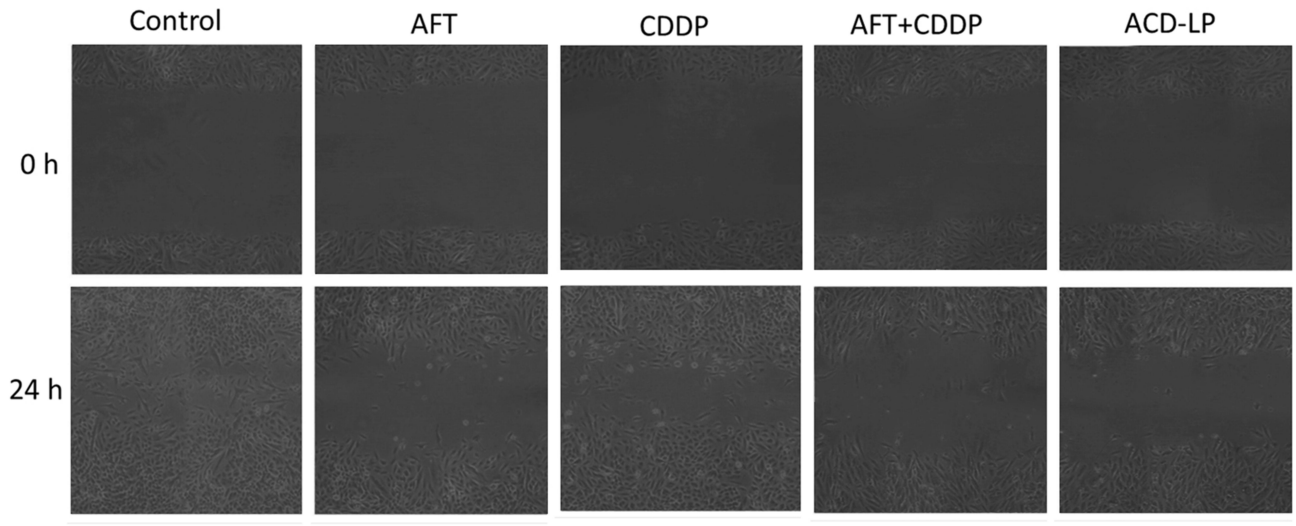

Figure 6 Migration of HONE1 cells after treatment with different formulations. Images were captured at 0 and 24 h using the Axiovert 200M microscope (Zeiss) equipped with the CoolSNAP ES camera.

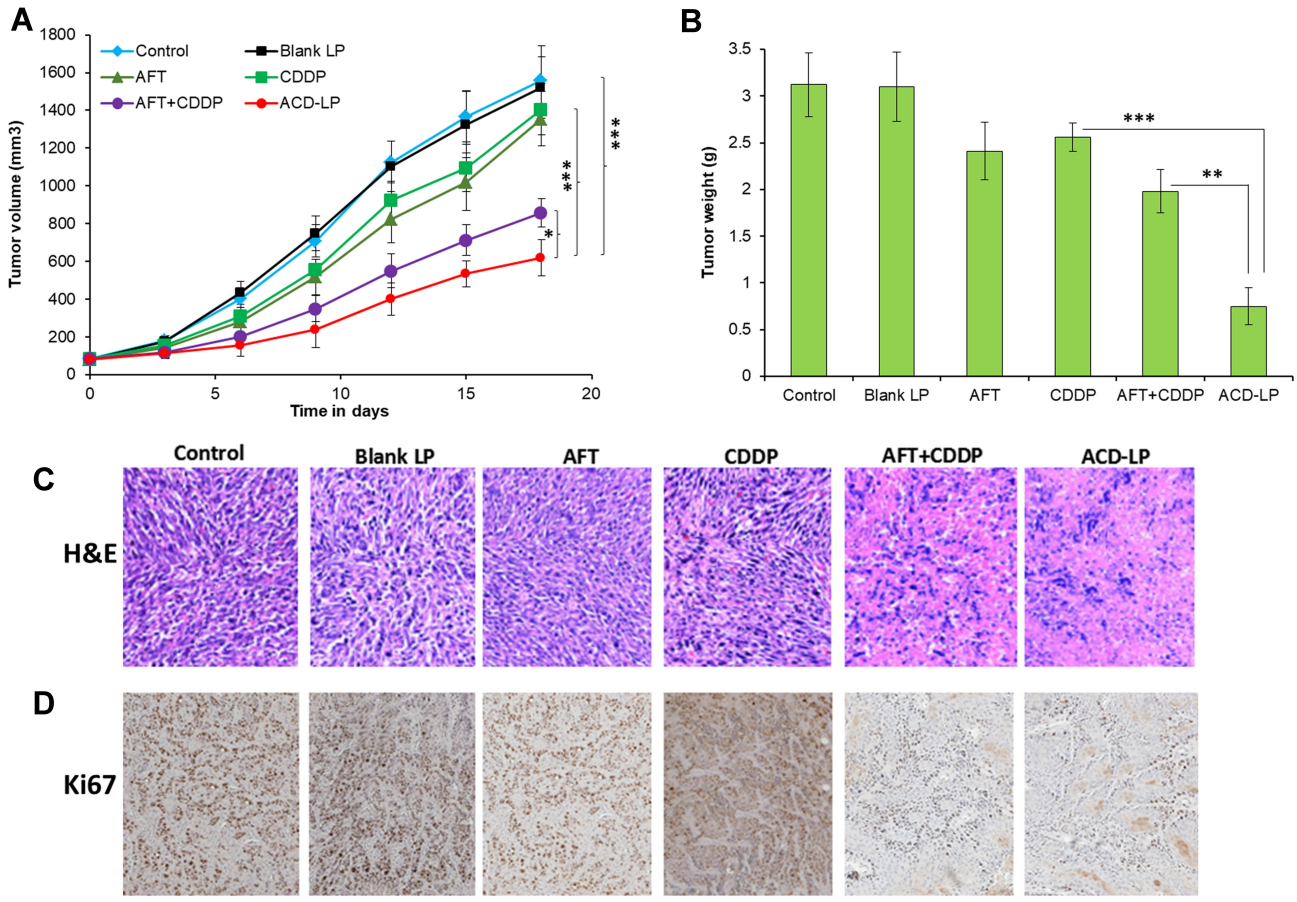

Figure 7 (**A**) Inhibition of tumor growth by different formulations in a nasopharyngeal carcinoma-bearing xenograft model. The groups included an untreated control group and groups given empty nanoparticles, the free drugs (alone or in combination), and cisplatin- and afatinib-loaded lipid–polymer hybrid nanoparticles. All formulations were given intravenously every third day (three injections). The data are means ± standard deviation. (**B**) The tumor weights. The data are means ± standard deviations. *p<0.05, **p<0.01 and ***p<0.0001 is the statistical difference. (**C** and **D**) Histochemical analysis of tumor tissues treated with different formulations.

monotherapies did not reduce the tumor volume. Combination CDDP+AFT and ACD-LP NPs significantly reduced the tumor volumes compared with the monotherapy and control groups. Tumor growth was significantly delayed in ACD-LP NP-treated mice. No significant difference in tumor volume was observed before day 6 between the CDDP+AFT and ACD-LP NP groups; however, the growth curves diverged by day 9 and remained significantly different until day 18, indicating the benefits of nanocarrier encapsulation and drug co-administration. The tumor volumes of the control, blank LP, AFT, CDDP, CDDP+AFT, and ACD-LP NP groups were 1558 ± 185, 1521 ± 161, 1356 ± 145, 1405 ± 135, 858 ± 75, and 619 ± 94 mm^3, respectively. The volumes of the tumors extracted after sacrifice exhibited a similar trend, with the ACD-LP NP group having the lowest tumor weight (0.75 ± 0.2 g) (Figure 7B). Tumor growth inhibition by ACD-LP NPs reflects the EPR effect; the NPs accumulated preferentially in tumor tissues. Importantly, NP formulations may maintain the drug ratios that are synergistic in vitro. Synergy between CDDP and AFT was crucial in terms of delaying tumor growth. When combined with CDDP, AFT decreased the levels of phospho-EGFR and phospho-HER2 and remarkably inhibited cancer cell proliferation and survival. Also, it is reasonable to expect that nanosized LP NPs may persist for some time in the circulation, facilitating tumor accumulation. In vivo toxicity was analyzed by monitoring the body weights of mice (Figure 8). Monotherapy (CDDP at 5 mg/kg) and the cocktail (CDDP+AFT) triggered significant weight loss (>10%) from days 3 to 9, indicating that the free drugs were severely toxic. In contrast, mice given ACD-LP NPs did not lose weight compared with the controls, suggesting beneficial effects of the NP system. Histological changes in tumor tissues were studied by using hematoxylin and eosin (H&E) staining. As shown, untreated cells maintained their shape and morphology, and no nuclear atypia were observed. The single drug-treated groups showed some decrease in tumor cell volume. Importantly, ACD-LP induced remarkable changes in tumor microstructures such as apoptotic condensations and marked fragmentation of cells. Tumor sections were further analyzed for Ki-67 expression, a tumor proliferation Immunohistochemical marker.[31] As seen from Figure 7C, ACD-LP-treatment significantly reduced Ki67-positive cancer cells, showing that ACD-LP remarkably

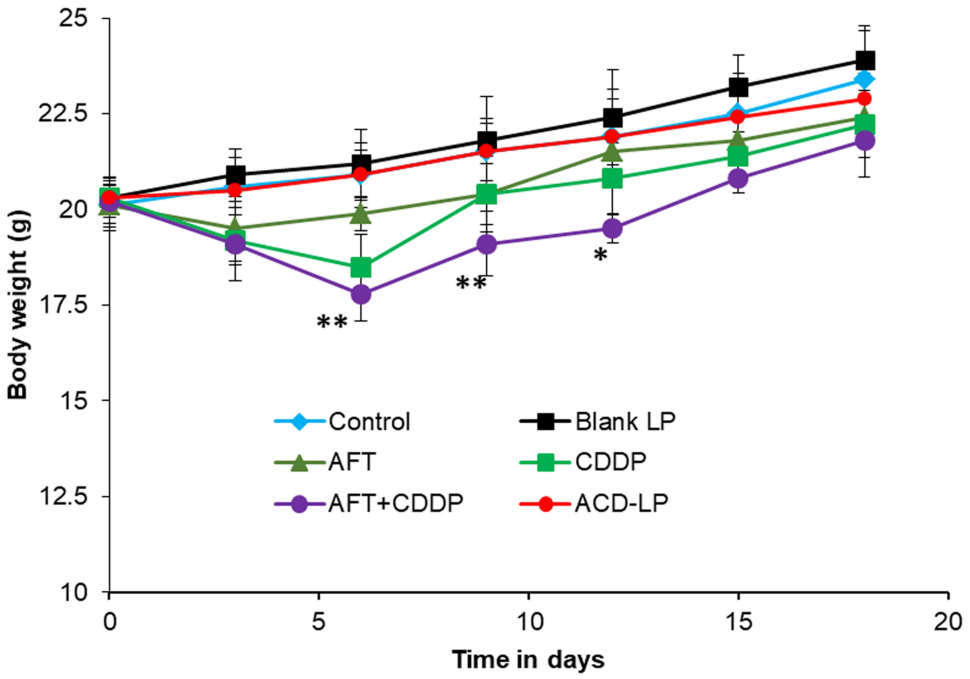

Figure 8 Body weights of tumor-bearing mice treated with different formulations. Mice were weighed daily until day 18 to monitor drug-induced toxicities. *p<0.05 is the statisitcal difference between AFT+CDDP vs ACD-LP. **p<0.05.

inhibited the proliferation of cancer cells. Overall, results clearly highlight the potential benefit of co-encapsulation of the two drugs in ACD-LP.

Conclusion

In this study, the antitumor effects of combination NPs (CDDP+AFT) were investigated using an NPC xenograft model. We demonstrated that CDDP and AFT exhibited synergistic anticancer activity at a specific molar ratio. The combination NPs exhibited enhanced therapeutic efficacy (compared with the free cocktail combination) in several in vitro experiments including cell viability, apoptosis, cell migration, and cell cycle analyses. The combination NPs significantly delayed tumor growth (with no obvious toxicity) compared with either CDDP or AFT monotherapy. Overall, the results suggest that LP NPs carrying CDDP and AFT exhibit great potential as an NPC treatment.

Acknowledgment

This study was supported by "The Application of OCT in Laryngology and Voice Science" program (grant no 14KG137).

Disclosure

The authors declare that they have no competing financial interests or conflicts of interest for this work.

References

1. Ferlay J, Soerjomataram I, Dikshit R, et al. Cancer incidence and mortality worldwide: sources, methods and major patterns in GLOBOCAN 2012. *Int J Cancer*. 2015;136(5):E359–E386. doi:10.1002/ijc.29210
2. Wei KR, Zheng RS, Zhang SW, Liang ZH, Ou ZX, Chen WQ. Nasopharyngeal carcinoma incidence and mortality in China in 2010. *Chin J Cancer*. 2014;33(8):381–387. doi:10.5732/cjc.014.10086
3. Lee HM, Okuda KS, González FE, Patel V. Current perspectives on nasopharyngeal carcinoma. *Adv Exp Med Biol*. 2019;1164:11–34.
4. Christodoulopoulos N, Mastronikolis N, Tsiambas E, et al. Impact of different therapeutic regimens on survival of patients with nasopharyngeal carcinoma. *J BUON*. 2019;24(6):2418–2422.
5. Ma BB, Hui EP, Chan AT. Systemic approach to improving treatment outcome in nasopharyngeal carcinoma: current and future directions. *Cancer Sci*. 2008;99(7):1311–1318. doi:10.1111/j.1349-7006.2008.00836.x
6. Ou D, Blanchard P, El Khoury C, et al. Induction chemotherapy with docetaxel, cisplatin and fluorouracil followed by concurrent chemoradiotherapy or chemoradiotherapy alone in locally advanced non-endemic nasopharyngeal carcinoma. *Oral Oncol*. 2016;62:114–121. doi:10.1016/j.oraloncology.2016.10.011
7. Zhang L, Huang Y, Hong S, et al. Gemcitabine plus cisplatin versus fluorouracil plus cisplatin in recurrent or metastatic nasopharyngeal carcinoma: a multicentre, randomised, open-label, Phase 3 trial. *Lancet*. 2016;388(10054):1883–1892. doi:10.1016/S0140-6736(16)31388-5
8. Maennling AE, Tur MK, Niebert M, et al. Molecular targeting therapy against EGFR family in breast cancer: progress and future potentials. *Cancers (Basel)*. 2019;11(12):1826. doi:10.3390/cancers11121826
9. Santos EDS, Nogueira KAB, Fernandes LCC, et al. EGFR targeting for cancer therapy: pharmacology and immunoconjugates with drugs and nanoparticles. *Int J Pharm*. 2021;592:120082. doi:10.1016/j.ijpharm.2020.120082
10. El Bezawy R, Cominetti D, Fenderico N, et al. miR-875-5p counteracts epithelial-to-mesenchymal transition and enhances radiation response in prostate cancer through repression of the EGFR-ZEB1 axis. *Cancer Lett*. 2017;395:53–62. doi:10.1016/j.canlet.2017.02.033
11. Morris ZS, Harari PM. Interaction of radiation therapy with molecular targeted agents. *J Clin Oncol*. 2014;32(26):2886–2893. doi:10.1200/JCO.2014.55.1366
12. Lee SC, Lim SG, Soo R, et al. Lack of somatic mutations in EGFR tyrosine kinase domain in hepatocellular and nasopharyngeal carcinoma. *Pharmacogenet Genomics*. 2006;16(1):73–74. doi:10.1097/01.fpc.0000184959.82903.02
13. Chua DT, Wei WI, Wong MP, Sham JS, Nicholls J, Au GK. Phase II study of gefitinib for the treatment of recurrent and metastatic nasopharyngeal carcinoma. *Head Neck*. 2008;30(7):863–867. doi:10.1002/hed.20792
14. Duru N, Fan M, Candas D, et al. HER2-associated radioresistance of breast cancer stem cells isolated from HER2-negative breast cancer cells. *Clin Cancer Res*. 2012;18(24):6634–6647. doi:10.1158/1078-0432.CCR-12-1436
15. Dokala A, Thakur SS. Extracellular region of epidermal growth factor receptor: a potential target for anti-EGFR drug discovery. *Oncogene*. 2017;36(17):2337–2344. doi:10.1038/onc.2016.393
16. Takezawa K, Pirazzoli V, Arcila ME, et al. HER2 amplification: a potential mechanism of acquired resistance to EGFR inhibition in EGFR-mutant lung cancers that lack the second-site EGFR T790M mutation. *Cancer Discov*. 2012;2(10):922–933. doi:10.1158/2159-8290.CD-12-0108
17. Bertotti A, Migliardi G, Galimi F, et al. A molecularly annotated platform of patient-derived xenografts ("xenopatients") identifies HER2 as an effective therapeutic target in cetuximab-resistant colorectal cancer. *Cancer Discov*. 2011;1(6):508–523. doi:10.1158/2159-8290.CD-11-0109
18. Lui VWY, Lau CPY, Ho K, et al. Anti-invasion, anti-proliferation and anoikis-sensitization activities of lapatinib in nasopharyngeal carcinoma cells. *Invest New Drugs*. 2011;29(6):1241–1252. doi:10.1007/s10637-010-9470-y
19. Liu L, Wang ZH, Han J, et al. Everolimus enhances cellular cytotoxicity of lapatinib via the eukaryotic elongation factor-2 kinase pathway in nasopharyngeal carcinoma cells. *Onco Targets Ther*. 2016;9:6195–6201. doi:10.2147/OTT.S115309
20. Zhou X, Shi K, Hao Y, et al. Advances in nanotechnology-based delivery systems for EGFR tyrosine kinases inhibitors in cancer therapy. *Asian J Pharm Sci*. 2020;15(1):26–41. doi:10.1016/j.ajps.2019.06.001
21. Katakami N, Atagi S, Goto K, et al. LUX-Lung 4: a phase II trial of afatinib in patients with advanced non-small-cell lung cancer who progressed during prior treatment with erlotinib, gefitinib, or both. *J Clin Oncol*. 2013;31(27):3335–3341. doi:10.1200/JCO.2012.45.0981
22. Dungo RT, Keating GM. Afatinib: first global approval. *Drugs*. 2013;73(13):1503–1515. doi:10.1007/s40265-013-0111-6
23. Ramasamy T, Ruttala HB, Gupta B, et al. Smart chemistry-based nanosized drug delivery systems for systemic applications: a comprehensive review. *J Control Release*. 2017;258:226–253.
24. Ramasamy T, Munusamy S, Ruttala HB, Kim JO. Smart nanocarriers for the delivery of nucleic acid-based therapeutics: a comprehensive review. *Biotechnol J*. 2021;16(2):e1900408. doi:10.1002/biot.201900408
25. Ruttala HB, Ramasamy T, Poudal BK, et al. Molecularly targeted co-delivery of a histone deacetylase inhibitor and paclitaxel by lipid-protein hybrid nanoparticles for synergistic combinational chemotherapy. *Oncotarget*. 2017;8(9):14925–14940. doi:10.18632/oncotarget.14742
26. Percie Du Sert N, Hurst V, Ahluwalia A, et al. The ARRIVE guidelines 2.0: updated guidelines for reporting animal research. *J Physiol*. 2020;598(18):3793–3801. doi:10.1113/JP280389

27. Longton E, Schmit K, Fransolet M, Clement F, Michiels C. Appropriate sequence for afatinib and cisplatin combination improves anticancer activity in head and neck squamous cell carcinoma. *Front Oncol*. 2018;8:Article 432. doi:10.3389/fonc.2018.00432
28. Huang F, Liang X, Min X, et al. Simultaneous inhibition of EGFR and HER2 via afatinib augments the radiosensitivity of nasopharyngeal carcinoma cells. *J Cancer*. 2019;10(9):2063–2207. doi:10.7150/jca.29327
29. Razumienko EJ, Chen JC, Cai Z, Chan C, Reilly RM. Dual-receptor-targeted radioimmunotherapy of human breast cancer xenografts in athymic mice coexpressing HER2 and EGFR using 177Lu- or 111In-labeled bispecific radioimmunoconjugates. *J Nucl Med*. 2015;57:444–452. doi:10.2967/jnumed.115.162339
30. Landgraf R. HER2 therapy. HER2 (ERBB2): functional diversity from structurally conserved building blocks. *Breast Cancer Res*. 2007;9(1):202. doi:10.1186/bcr1633
31. Ramasamy T, Chen X, Qin B, Johnson DE, Grandis JR, Villanueva FS. STAT3 decoy oligonucleotide-carrying microbubbles with pulsed ultrasound for enhanced therapeutic effect in head and neck tumors. *PLoS One*. 2020;15(11):e0242264. doi:10.1371/journal.pone.0242264